CrystEngComm

Effect of growth temperature conditions on the optimization of OH1 single-crystalline thin film by physical vapour deposition

Journal:	*CrystEngComm*
Manuscript ID	CE-ART-10-2019-001598.R1
Article Type:	Paper
Date Submitted by the Author:	07-Nov-2019
Complete List of Authors:	Wang, Pei-bin; Nagoya University Takeya, Kei; Nagoya University Kawase, Kodo; Nagoya University Uchida, Hirohisa ; Nagoya University; Arkray Inc

ARTICLE

Effect of growth temperature conditions on the optimization of OH1 single-crystalline thin film by physical vapour deposition

Received 00th January 20xx,
Accepted 00th January 20xx

DOI: 10.1039/x0xx00000x

Pei-bin Wang, [a] Kei Takeya, *[a] Kodo Kawase, [a] and Hirohisa Uchida *[a,b]

2-(3-(4-hydroxystyry1)-5,5-dimethylcyclohex-2-enylidene malononitrile (OH1) is the only organic nonlinear optical (NLO) crystal that can be crystallized by physical vapour deposition (PVD) for terahertz (THz) wave generation. We report some optimizations of the growth temperature conditions of single-crystalline thin film by PVD. After transforming the setting temperature conditions from 90-120-180 °C to 90-145-180 °C, we observed that the temperature conditions influence the size of the OH1 single-crystalline thin film. Moreover, we found that, when the temperature gradient conditions were held at 90-135-180 °C during PVD for the growth of OH1 single-crystalline thin film, the single-crystalline thin films had longer b-axial extensions, which may be better-suited to nonlinear optics. The infrared transmission spectroscopy absorption peak positions of the OH1 single-crystalline thin film fabricated in this study were the same as those of bulk OH1 crystal. The crystallinity of the OH1 single-crystalline thin film was higher than that of bulk OH1 crystal, under all temperature conditions.

Introduction

Organic nonlinear optical crystal OH1.

Nonlinear optical (NLO) crystal is a superior material widely used for wavelength conversion. Among NLO crystals, organic NLO crystals have higher NLO coefficients than inorganic NLO crystals.[1-3] 2-(3-(4-hydroxystyry1)-5,5-dimethylcyclohex-2-enylidene malononitrile (OH1) is a type of organic NLO crystal that has a high nonlinear coefficient (d33 = 120 pm/V@1.9 μm).[4, 5] Therefore, OH1 crystals are expected to find applications in various optical devices.[6, 7]

Terahertz generation using nonlinear optical crystals.

An effective application of nonlinear optical crystals is terahertz (THz) wave generation and detection. THz waves are electromagnetic waves with frequencies from 100 GHz to 10 THz, i.e., between radio waves and light waves. Several unique applications of THz waves are currently under development.[8, 9] In particular, there are many applications based on THz time-domain spectroscopy (THz-TDS), such as high-resolution tomography,[10] measurement of tablet-coating thickness,[11] determination of chloride ion concentrations in concrete,[12] and communications.[13] Many studies on THz sources using various NLO crystals have been performed, and they can generate THz waves efficiently, with relative ease. However, we must improve the performance of THz sources before they can be used to make advanced measurements.[14-18]

In previous studies, we investigated organic NLO crystals in terms of THz generation using the prism-coupled Cherenkov phase-matching (PCC-PM) method.[19-22] This method enables us to generate coherent THz waves along the Cherenkov angle, and therefore suppress absorption of the NLO crystal.[23-25] However, the thickness of the NLO crystal can cause phase mismatches when using the PCC-PM method.[26, 27] The generated THz waves interfere with and cancel each other out, because of their different points of generation. We can solve the phase mismatch using a thin crystal.[26, 28] Regarding the crystal shape, the result given by Lee showed a large crystal with an area of ~600 mm^2 has been grown from a 0.2 mm-thick OH1 seed with an area of 3.5 mm^2 with a method of solution evaporation.[29] The phenolic polyene OH1 crystals with higher purity and better optical quality have been achieved by using a particular ionic organic addictive from the results of Choi's report.[30] The growth of OH1 thin film crystals by evaporation-induced local supersaturation method has been reported by Kwon.[31] However, according to the former methods, it is not easy to design a shape of organic NLO crystals, due to mechanical fragility, the solubility of organic crystals and other problems.[2] As described above, the shape control of organic nonlinear optical crystals is very important to increase the optical applicability.

Optimize the condition of OH1 crystallization by PVD.

Recently, we developed an easy physical vapour deposition (PVD) method to grow OH1 single-crystalline thin films, via which we achieved successful THz generation.[7] In previous studies, employing a PVD setting temperature gradient of 90-120-180 °C, we obtained single-crystalline thin film with a width of hundreds of μm. The width of the OH1 thin film crystal represents the b-axial extension. In this study, the

[a] Department of Electronics, Nagoya University, Nagoya, 464-8603, Japan.
[b] ARKRAY Inc., Kamigyo-ku, Kyoto 602-0008, Japan.
* Kei Takeya. takeya@nuee.nagoya-u.ac.jp,
* Hirohisa Uchida. uchidah@arkray.co.jp

shape of the OH1 single-crystalline thin film is controlled by the growth conditions. The temperature gradient of the PVD affects the crystal size by influencing the convection and deposition rates of OH1 gas molecules. Therefore, we varied the temperature settings to identify the best temperature gradient for the growth of OH1 single-crystalline thin films with a long b-axial extension, and appealing crystal shape and habit.

Experiments

The schematic diagram of the PVD experiment for fabricating OH1 single-crystalline thin film is shown in Figure 1.

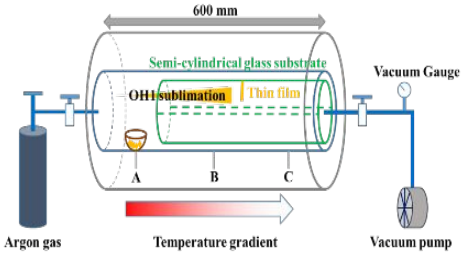

Figure 1. Schematic of the physical vapour deposition (PVD) apparatus. OH1 crystal powder is heated in a tubular furnace with temperature gradient A-B-C, and sublimated; it then crystalizes at the glass substrate.

A tubular furnace with a three-zone temperature gradient (A-B-C), from high to low. The OH1 powder was placed in section A of the tubular furnace, and two pieces of semi-cylindrical glass substrate were inserted into sections B and C. By using cocks and a vacuum pump, we reduced the pressure inside the tubular furnace to a vacuum, and then implanted Argon gas to maintain the pressure at 0.07 MPa. The heating time of the tubular furnace was 24 hours under every temperature condition tested.

At first the high temperature section A was investigated based on our previous research.7 By thermogravimetry and differential thermal analysis measurements of powdered OH1 crystals, the endothermic peak was observed 212 °C, near the melting point. Moreover, the weight of OH1 gradually decreased from 100 °C to 190 °C at atmospheric pressure. Conversely, when temperature condition was set at 185-120-90 °C, the OH1 powder turned black because of pyrolysis after 24h crystallization experiment. Therefore, the high temperature section A was determined at 180 °C to sublimate at a temperature as high as possible.

The temperature of section C was investigated by X-ray diffraction (XRD) measurement. The growth of the OH1 single crystal thin film used for the evaluation was varied the temperature of section C from 30 °C to 100 °C. Then, sections A and B were set to the conditions where temperatures were kept at 180 ° C and 120 ° C, respectively. The X-ray diffraction patterns of OH1 single-crystalline thin films grown under different temperature conditions were obtained from out-of-plane measurements (2θ/ω-scan) and X-ray rocking curve measurements (ω-scan) in the *bc*-plane using a thin film X-ray diffraction device (ATX-G; RIGAKU). The device used a Cu-Kα1 source and its highest power was 18 kW. The voltage and current in this experiment were set to 50 kV and 300 mA, respectively. The diffraction of the OH1 crystal was recorded at 0.001 deg intervals, from 10 to 40 deg, ±0.2 deg from the peak position. Figure 2 is shown the XRD measurement results. A full width half maximum by rocking curve measurement of OH1 single crystalline thin films were decreased that as temperature increases. In addition, when the temperature of section C exceeded 100 ° C, only microcrystals that were not suitable for THz wave generation were grown. When the temperature of section C is about the same as that of section B, OH1 molecules were less likely to aggregate, which suppresses crystal growth. Conversely, when the temperature of section C is extremely lower than the temperature of section B, the two-dimensional nucleation was excessively grown, so that the grown thin films were considered to be polycrystalline or low-oriented. In the fact, the full width at half maximum by rocking curve measurement of OH1 single-crystalline thin films were depended on the temperature of section C. Therefore, sections C was set to 90 °C.

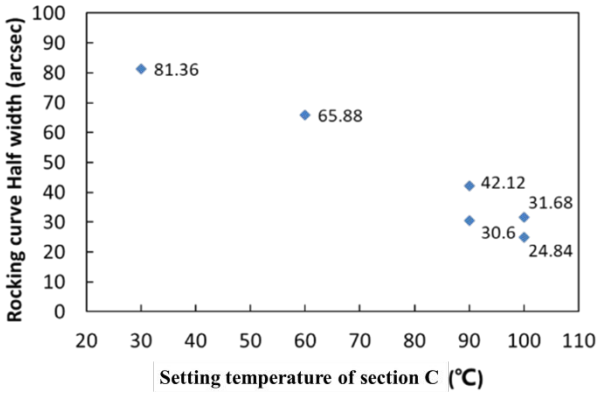

Figure 2. X-ray rocking curve measurement results of OH1 single-crystalline thin films grown under different temperature conditions of section C. The temperature of section A and B were 180 °C and 120 °C, respectively.

The temperature of B was varied from 120 °C to 145 °C as shown in Table 1. The spatial distribution of the growth of the OH1 crystal on the glass substrate, and the size of each crystal, was measured using a microscope (VW-6000; KEYENCE).

Table 1. Setting growth temperature conditions of PVD in this study

	A (°C)	B (°C)	C (°C)
I	180	120	90
II	180	125	90
III	180	130	90
IV	180	135	90
V	180	140	90
VI	180	145	90

Figure 3 shows the actual temperature gradient of the OH1 single-crystalline thin film crystallization environment, measured by installing several thermocouple sensors inside the tubular furnace. There are similar temperatures at the A

section around 185 °C and C section around 95 °C in the tubular furnace. But the temperature conditions I-VI have considerably different values at the B section from 129 °C to 150 °C. And there are also deviations between setting temperatures and actual temperatures. The actual temperature conditions were utilized to explain the effect of growth temperature conditions on the optimization of OH1 single-crystalline thin film by physical vapour deposition.

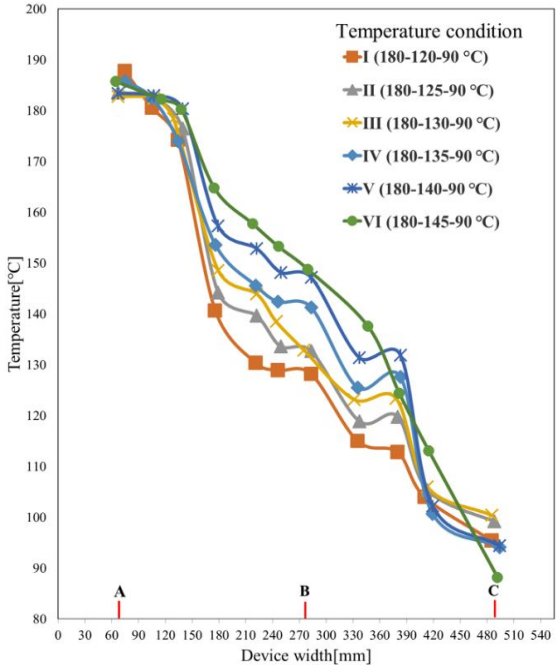

Figure 3. The measurement temperature gradient in the tubular furnace. The red lines at A, B and C show the locations of the PVD thermocouple sensors.

The Fourier transform infrared (FTIR) spectra of the OH1 single-crystalline thin films were measured by micro-Fourier transform infrared spectroscopy (FT/IR6100; JASCO Corporation) at room temperature. The spectra were recorded at 1.92847 cm^{-1} intervals, from 399.193 cm^{-1} to 8,001.21 cm^{-1}. The FTIR spectra of OH1 bulk crystal were also measured for comparison and reference. The thickness of the OH1 bulk crystal was approximately 600 µm and that of the thin film crystal was 8 µm.

Results and discussion

Effect of temperature gradient on the shape of crystals.

Using a polarizing microscope, we observed that the size of the OH1 single-crystalline thin films varied with the growth temperature conditions in the tubular furnace. Images of six OH1 single-crystalline thin film are shown in Figure 4. While many crystals were fabricated under each temperature condition, the photograph in Figure 4 shows those with large distributions between them (see also Figure 6). We can clearly see that the sizes of the crystals vary with temperature, and the crystals created under temperature conditions III (B: 130°C) and IV (B: 135°C) were wider than the other crystals (Figure 4). The obtained OH1 single-crystalline thin films were

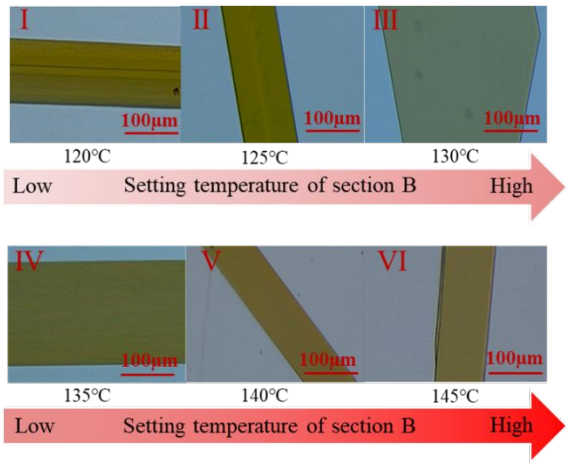

Figure 4. Images of OH1 single-crystalline thin films grown under six conditions. All pictures have the same scale.

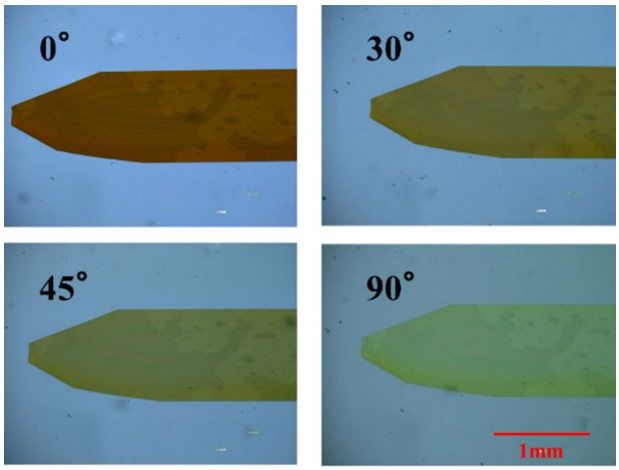

Figure 5. Optical micrographs of an OH1 single-crystalline thin film with a polarized light source at 0, 30, 45 and 90 degrees.

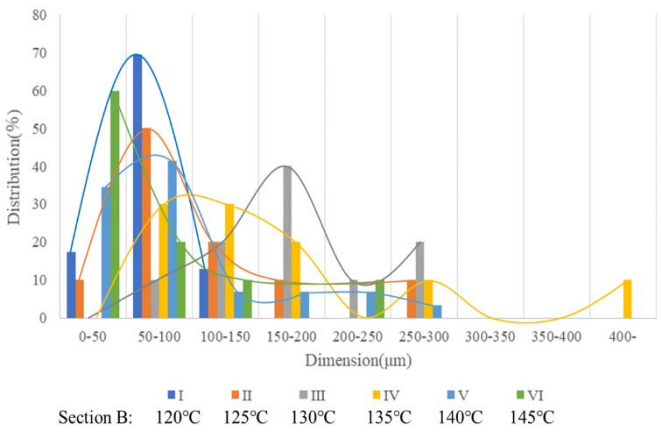

Figure 6. Distribution of the b-axial dimension categories of OH1 crystals obtained under different temperature conditions.

single crystals, as shown by their uniform polarization characteristics (Figure 5). The obtained OH1 single-crystalline thin films were of optical quality and had a much longer extension in the b-axis direction under temperature condition

IV (B: 135°C). The longer extension along the b-axis allows for ample interaction between the pump laser and the crystal for THz generation. Thus, the shape of the obtained OH1 single-crystalline thin film under condition IV (B:135°C) should be suitable as a THz source.

To confirm the effect of the growth temperature conditions, we calculated the distributions of b-axial dimension categories of the OH1 crystals under different temperature conditions, as shown in Figure 6; the distributions varied among temperature conditions. We can see that, under conditions I (B: 120°C), II (B: 125°C), V (B: 140°C), and VI (B: 145°C), b-axial dimensions were mostly in the range of 0-100 μm, i.e., most of the OH1 single-crystalline thin films had b-axial dimensions of no more than 100 μm. Meanwhile, under temperature conditions III (B: 130°C) and IV (B: 135°C) many thin films had b-axial

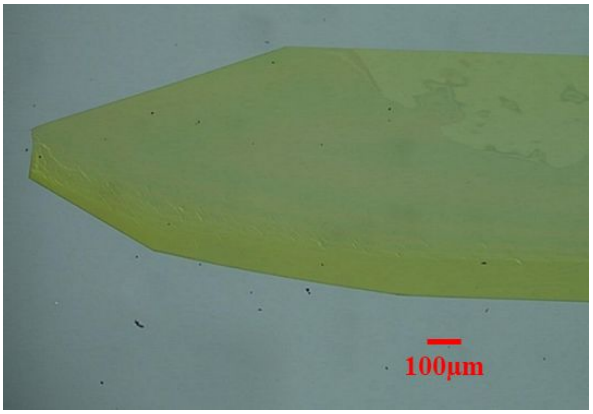

Figure 7. Image of an OH1 single-crystalline thin film grown under temperature condition IV.

dimensions over 100 μm. Under condition IV (B: 135°C), we obtained an OH1 single-crystalline thin film with the largest b-axial dimension (974.97 μm) achieved thus far (Figure 7).

Section B along the temperature gradient (see Figure 3) is the point at which there is a switch from slow to rapid cooling. Substantial amounts of droplet-like amorphous material adhered to the substrate when the switch point occurred at less than 140 ° C, while many microcrystals were grown on the substrate when the switch point exceeded 140 ° C. Under all temperature conditions, the temperature at section A, where the crucible was placed, was 180 ° C, and the heating time was 24 hours. Hence, the mass of evaporated OH1 molecules was the same under all temperature conditions. We suggest that the PVD of OH1 depends largely on the temperature switch point and the phase; when the switch point was 140 ° C, the single-crystalline thin film extended along the b-axis. This confirms experimentally that two-dimensional nucleation and crystal growth were in balance at 140 ° C.

The average growth velocity of OH1 single-crystalline thin film at each condition was calculated by the b-axial dimension distribution data, shown in Figure 8. It can be observed that OH1 single-crystalline thin films has the highest growth velocity relatively at condition IV (B: 135°C). When the temperature of section B increases, the temperature gradient from section A to section B turns slower. This results in the local residence time extension of OH1 molecule, so the growth velocity gradually increases as B temperature increases. However, when it exceeds condition IV, the environment temperature is too high for OH1 molecules to aggregate and we can just get some microcrystals.

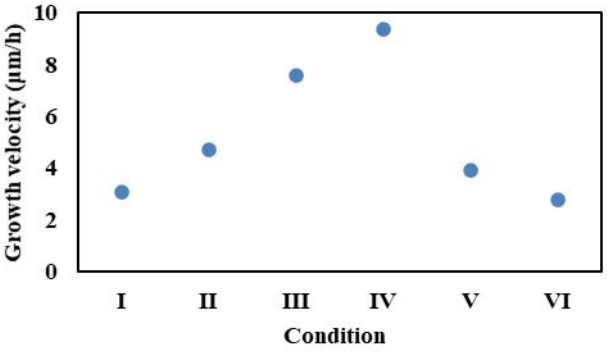

Figure 8. The average growth velocity in the b-axis direction of OH1 single-crystalline thin film at each condition.

Here, it can be assumed that the diffusion rates of gas molecules in the tubular furnace, and the local residence time and concentration distribution, vary depending on the temperature conditions in the furnace at section B. The temperature difference at a furnace of approximately 150 mm, shown in Figure 3, affected the magnitude of the convection and velocity of the gas molecules. Furthermore, the locations of the gas molecules may vary depending on the temperature distribution around section B. Efficient crystal growth occurs when the area in which OH1 molecules gather has a temperature of approximately 140 ° C, and we can assume that a difference in crystal growth will be seen at other temperatures.

Infrared transmission spectroscopy of OH1 bulk crystal and thin film crystal.

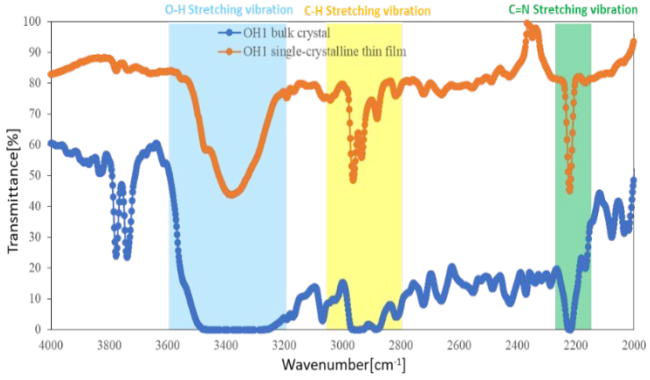

Figure 9. Infrared transmission spectroscopy results of OH1 bulk and thin film crystals.

We carried out infrared transmission spectroscopy in the 4,000 to 2,000 cm-1 region of the OH1 bulk and thin film crystals, as shown in Figure 9. The blue, orange, and green areas are the regions of O-H stretching vibrations at 3,400 to 3,500 cm-1, C-H stretching vibrations at 3,000 cm-1, and C≡N

stretching vibrations at 2,200 cm-1, respectively. The absolute absorption values of the OH1 bulk crystal are greater than those of the OH1 single-crystalline thin film, because the OH1 bulk crystal has a thickness of 600 µm, which is about 70 times greater than that of OH1 single-crystalline thin film (thickness of 8 µm). This result is compatible with those calculated based on the Lambert-Beer law. However, there were no differences in the positions of the peaks of the IR spectra between the OH1 bulk crystal and thin film. Therefore, it appears that OH1 single-crystalline thin film grown by PVD has the same molecular structure as OH1 bulk crystal.

X-ray diffraction analysis of OH1 crystals grown under different conditions.

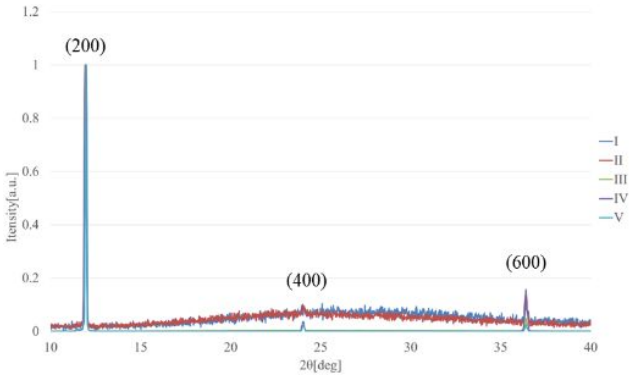

Figure 10. X-ray diffraction patterns of OH1 single-crystalline thin films grown under different temperature conditions (I–V).

Figure 10 shows the XRD patterns of OH1 single-crystalline thin films grown by PVD under different temperature conditions (I–V); the patterns were obtained from out-of-plane measurements (2θ/ω-scan) in the *bc*-plane. Under all temperature conditions, peaks occurred at the same positions in the (200), (400), and (600) planes. Thus, we demonstrated that OH1 single-crystalline thin films grown under different temperature conditions have the same lattice constant in the a-axis.

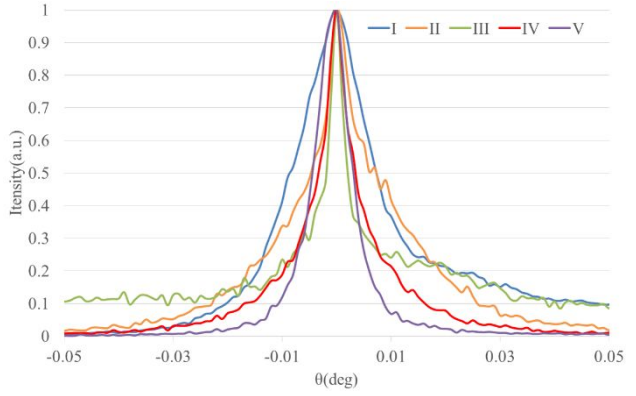

Figure 11. X-ray rocking curve measurements (ω-scan), for OH1 single-crystalline thin film grown under five different temperature conditions.

The results of X-ray rocking curve measurements (ω-scan), for OH1 single-crystalline thin films grown under five different temperature conditions, are shown in Figure 11. The full width at half-maximum (FWHM) of OH1 single-crystalline thin film under temperature condition I–V is 59.76 arcsec, 30.6 arcsec, 13.68 arcsec, 24.28 arcsec, 14.4 arcsec respectively, and the FWHM of the bulk crystal is 59 arcsec measured by our previous work,[1] which is greater than those of the thin films grown under temperature conditions II–V. When the setting temperature at section B was increased from 120 °C to 135 °C, we obtained OH1 single-crystalline thin film with longer b-axial dimensions, which were more suitable for THz generation. Moreover, the FWHM of the OH1 single-crystalline thin film was lower compared to bulk crystals and previously reported thin films. The results showed that, for the OH1 single-crystalline thin film, temperature condition IV yielded a crystalline perfection equivalent to, or better than, that obtained under the conditions used in previous studies, and of other films fabricated using conventional crystal growth methods. We will be able to obtain OH1 single-crystalline thin films with the optimum shape according to the purpose by the growth temperature conditions.

Conclusions

We investigated the optimization of temperature conditions for PVD growth of OH1 crystal. As a result, we achieved control over the growth of OH1 single-crystalline thin film simply by changing the temperature conditions. By setting the temperature gradient of PVD to 90-135-180 °C, a high crystallinity OH1 single-crystalline thin film with long extension along the b-axis was obtained. We analysed the fabricated samples using infrared spectroscopy and XRD, and observed that the OH1 thin film crystal obtained by vapour phase growth has higher crystallinity than the bulk crystal. To obtain a large and high crystallinity OH1 single-crystalline thin film in the b-axis direction, it is extremely important to maintain the actual temperature of section B at 140 °C. This confirms experimentally that two-dimensional nucleation and crystal growth were in balance at 140 ° C.

Conflicts of interest

There are no conflicts to declare.

Acknowledgements

We acknowledge the contributions of K. Okimura of Nagoya University for his experimental support and helpful discussion, and Prof. Tatsuo Mori of Aichi Institute of Technology for his advice related to the development of single-crystalline thin films.

References

1. H. Nakanishi, H. Matsuda, S. Okada and M. Kato, Organic polymeric ion-complexes for nonlinear optics. *Proc. MRS Int. Meet. Adv. Mater.* 1989, **1**, 97.
2. M. Jazbinsek, L. Mutter and P. Gunter, *IEEE Journal of selected topics in quantum electronics*, 2008, **14**, 1298-1311.
3. H. Ito, K. Suizu, T. Yamashita, A. Nawahara and T. Sato, *Japanese Journal of Applied Physics*, 2007, **46**, 7321.
4. C. Hunziker, S.-J. Kwon, H. Figi, F. Juvalta, O.-P. Kwon, M. Jazbinsek and P. Günter, *JOSA B*, 2008, **25**, 1678-1683.
5. C. Vicario, M. Jazbinsek, A. Ovchinnikov, O. Chefonov, S. Ashitkov, M. Agranat and C. Hauri, *Optics express*, 2015, **23**, 4573-4580.
6. F. D. Brunner, O.-P. Kwon, S.-J. Kwon, M. Jazbinšek, A. Schneider and P. Günter, *Optics express*, 2008, **16**, 16496-16508.
7. H. Uchida, R. Yamazaki, K. Oota, K. Okimura, T. Minami, K. Takeya and K. Kawase, *Crystal Growth & Design*, 2018, **18**, 4029-4036.
8. M. Tonouchi, *Nature photonics*, 2007, **1**, 97.
9. B. Ferguson and X.-C. Zhang, *Nature materials*, 2002, **1**, 26.
10. J. Takayanagi, H. Jinno, S. Ichino, K. Suizu, M. Yamashita, T. Ouchi, S. Kasai, H. Ohtake, H. Uchida and N. Nishizawa, *Optics express*, 2009, **17**, 7533-7539.
11. A. J. Fitzgerald, B. E. Cole and P. F. Taday, *Journal of pharmaceutical sciences*, 2005, **94**, 177-183.
12. S. R. Tripathi, H. Ogura, H. Inoue, T. Hasegawa, K. Takeya and K. Kawase, *Corrosion Science*, 2012, **62**, 5-10.
13. T. Kleine-Ostmann and T. Nagatsuma, *Journal of Infrared, Millimeter, and Terahertz Waves*, 2011, **32**, 143-171.
14. D. H. Auston and M. C. Nuss, *IEEE Journal of quantum electronics*, 1988, **24**, 184-197.
15. J. Hebling, K.-L. Yeh, M. C. Hoffmann, B. Bartal and K. A. Nelson, *JOSA B*, 2008, **25**, B6-B19.
16. H. Hirori, A. Doi, F. Blanchard and K. Tanaka, *Applied Physics Letters*, 2011, **98**, 091106.
17. J. Hebling, G. Almasi, I. Z. Kozma and J. Kuhl, *Optics Express*, 2002, **10**, 1161-1166.
18. K. Takeya, K. Suizu, H. Sai, T. Ouchi and K. Kawase, *IEEE Journal of Selected Topics in Quantum Electronics*, 2012, **19**, 8500212-8500212.
19. K. Suizu, T. Shibuya, T. Akiba, T. Tutui, C. Otani and K. Kawase, *Optics express*, 2008, **16**, 7493-7498.
20. K. Suizu, K. Koketsu, T. Shibuya, T. Tsutsui, T. Akiba and K. Kawase, *Optics express*, 2009, **17**, 6676-6681.
21. H. Uchida, K. Oota, T. Minami, K. Takeya and K. Kawase, *Applied Physics Express*, 2017, **10**, 062601.
22. K. Takeya, K. Okimura, K. Oota, K. Kawase and H. Uchida, *Optics letters*, 2018, **43**, 4100-4103.
23. K. Chikuma and S. Umegaki, *JOSA B*, 1990, **7**, 768-775.
24. T. Shibuya, T. Tsutsui, K. Suizu, T. Akiba and K. Kawase, *Applied Physics Express*, 2009, **2**, 032302.
25. S. R. Tripathi, K. Murate, H. Uchida, K. Takeya and K. Kawase, *Applied Physics Express*, 2013, **6**, 072703.
26. S. Fan, H. Takeuchi, T. Ouchi, K. Takeya and K. Kawase, *Optics letters*, 2013, **38**, 1654-1656.
27. K. Takeya, T. Minami, H. Okano, S. Tripathi and K. Kawase, *APL Photonics*, 2017, **2**, 016102.
28. H. Uchida, K. Oota, K. Okimura, K. Kawase and K. Takeya, *Journal of Infrared, Millimeter, and Terahertz Waves*, 2018, **39**, 509-513.
29. S. H. Lee, S. J. Lee, M. Jazbinsek, B. J. Kang, F. Rotermund and O. P. Kwon, *CrystEngComm*, 2016, **18**, 7311-7318.
30. E. Y. Choi, M. Jazbinsek, J. H. Jeong and O.P Kwon, *CrystEngComm*, 2012, **14**, 1045.
31. S. J. Kwon, C. Kunziker, O. P. Kwon, M. Jazbinsek, P. Günter, *Crystal Growth & Design*, 2009, **9**, 2512-2516.